Draft version February 2, 2008
Preprint typeset using LaTeX style emulateapj v. 11/12/01

arXiv:astro-ph/0403095v3 9 Sep 2004

# DIFFUSIVE PROPAGATION OF UHECR AND THE PROPAGATION THEOREM

R. Aloisio and V. Berezinsky
INFN - Laboratori Nazionali del Gran Sasso, I–67010 Assergi (AQ), Italy
aloisio@lngs.infn.it, berezinsky@lngs.infn.it
*Draft version February 2, 2008*

## ABSTRACT

We present a detailed analytical study of the propagation of ultra high energy (UHE) particles in extragalactic magnetic fields. The crucial parameter which affects the diffuse spectrum is the separation between sources. In the case of a uniform distribution of sources with a separation between them much smaller than all characteristic propagation lengths, the diffuse spectrum of UHE particles has a *universal* form, independent of the mode of propagation. This statement has a status of theorem. The proof is obtained using the particle number conservation during propagation, and also using the kinetic equation for the propagation of UHE particles. This theorem can be also proved with the help of the diffusion equation. In particular, it is shown numerically, how the diffuse fluxes converge to this universal spectrum, when the separation between sources diminishes. We study also the analytic solution of the diffusion equation in weak and strong magnetic fields with energy losses taken into account. In the case of strong magnetic fields and for a separation between sources large enough, the GZK cutoff can practically disappear, as it has been found early in numerical simulations. In practice, however, the source luminosities required are too large for this possibility.

*Subject headings:* UHE Cosmic rays, propagation of cosmic rays, GZK cutoff.

## 1. INTRODUCTION

The propagation of UHECR protons and nuclei with $E \gtrsim 1 \times 10^{19}$ eV in the large-scale intergalactic magnetic field (IMF) remains an open problem, mainly because the knowledge of the IMF is still very poor. The possibilities vary between rectilinear propagation in a weak field and diffusive propagation in a strong magnetic field. The experimental data on IMF and the models of origin of these fields do not allow at present to choose even between the two extreme propagation regimes mentioned above.

Most reliable observations of the intergalactic magnetic field are based on the Faraday rotation of the polarized radio emission (for the reviews see Kromberg (1994), Vallé (1997), Carilli and Taylor (2002)) . The upper limit on the Faraday rotation measure (RM) in the extragalactic magnetic field, obtained from the observations of distant quasars, gives an upper limit of RM $< 5$ rad/m$^2$. It implies an upper limit on the extragalactic magnetic field on each assumed scale of coherence length (Kromberg (1994), Vallè (1997), Ryu et al. (1998)). For example, according to Blasi et al. (1999a) for an inhomogeneous universe $B_{l_c} < 4$ nG on a scale of coherence $l_c = 50$ Mpc.

According to observations of the Faraday rotations the extragalactic magnetic field is strongest, or order of 1 $\mu$G, in clusters of galaxies and radiolobes of radiogalaxies (Vallé (1997), Kromberg (1994), Carilli and Taylor (2002)). The largest scale in both structures reaches $l_c \sim 1$ Mpc. Most probably various structures of the universe differ dramatically by magnetic fields, with very weak field in voids and much stronger in the filaments (Ryu et al. (1998)). Superclusters seem to be too young for the regular magnetic field to be formed in these structures on a large scale $l_c \sim 10$ Mpc.

In case of hierarchical magnetic field structures in the universe, UHE protons with $E > 4 \times 10^{19}$ eV can propagate in a quasi-rectilinear regime. Scattering of UHE protons occurs mostly in galaxy clusters, radiolobes and filaments. Deflections of UHE protons can be large for some directions and small for the others. The universe looks like a leaky, worm-holed box, and correlation with the sources can be observable (see Tinyakov and Tkachev (2001)), where correlations of UHECR with BLLacs are found). Such a picture has been suggested by Berezinsky et al. (2002b).

A promising theoretical tool to predict the IMF in large scale structures is given by magneto-hydrodynamic (MHD) simulations. The main uncertainty in these simulations is related to the assumptions concerning the seed magnetic field.

The MHD simulations of Sigl et al. (2004) and Sigl et al. (2003) favor the hierarchical structure with strong magnetic fields. Assuming an inhomogeneous seed magnetic field generated by cosmic shocks through the Biermann battery mechanism, the authors obtain a $\sim 100$ nG magnetic field in filaments and $\sim 1$ nG in voids. In some cases they consider IMF up to a few micro Gauss as allowed. In these simulations UHECR are characterized by large deflection angles, of the order of 20°, at energies up to $E \sim 10^{20}$ eV (Sigl et al. (2003), Sigl et al. (2004)). Thus, the scenario that emerges in these simulations seems to exclude the UHECR astronomy. These simulations have some ambiguity related to the choice of magnetic field at the position of the observer (Sigl et al. (2003), Sigl et al. (2004)). The authors consider two cases: a strong local magnetic field $B \sim 100$ nG and a weak field $B \ll 100$ nG. The different assumptions about the local magnetic field strongly affects the conclusions about UHECR spectrum and anisotropy.

The essential step forward in MHD simulations has been made recently. In Dolag et al. (2003) the Local Universe is simulated with the observed density and velocity field. This eliminates the ambiguity for the local magnetic field, that is found to be weak. The seed magnetic field, used in this simulation, is normalized by the observed magnetic field in

rich clusters of galaxies. The results of these constrained simulations indicate the weak magnetic fields in the universe of the order of 0.1 nG in typical filaments and of 0.01 nG in voids. The strong large-scale magnetic field, $B \sim 10^3$ nG, exists in clusters of galaxies, which, however, occupy insignificant volume of the universe. The picture that emerges from simulations of Dolag at el. (2003) favors a hierarchical magnetic field structure characterized by weak magnetic fields. UHE protons with $E > 4 \times 10^{19}$ eV can propagate in a quasi-rectilinear regime, with the expected deflection angles being very small $\leq 1^\circ$. However, until direct observational evidences for this picture becomes available, an alternative case of propagation in strong magnetic fields, with diffusion as an extreme possibility, can be hardly excluded.

This case has been studied in Sigl et al. (1999), Lemoine et al. (1999), Stanev (2000), Harari et al. (2002), Yoshiguchi et al. (2003), Deligny et al. (2003). An interesting features found in these calculations are small-angle clustering of UHE particles as observed by Hayashida et al. (1996), Hayashida et al. (1999), Uchiori et al. (2000), Glushkov and Pravdin (2001), and absence of the GZK cutoff in the diffusive propagation, when the magnetic field is very strong. Many aspects of diffusion of UHECR have been studied in numerical simulation by Casse et al. (2002).

We shall illustrate UHECR propagation in strong magnetic fields by the calculations by Yoshiguchi et al. (2003). The authors performed MC simulations for propagation in random magnetic field with the Kolmogorov spectrum of turbulent energy density $w_k \propto k^n$, with $n = -5/3$. The basic (largest) coherent scale is chosen as $l_c$ with the mean field $B_0$. Numerically these parameters vary in the range (1 - 40) Mpc for $l_c$, and (1 - 100) nG - for $B_0$. The sources are taken as galaxies from Optical Redshift Survey catalog with absolute magnitude $M_B$ brighter than some critical value $M_c$. The calculated quantities are the energy spectrum, anisotropy and small-angle clustering. The observed small-angle clustering and absence of the GZK cutoff in the AGASA observations can be reproduced in the case of strong magnetic field $B \geq 10$ nG.

Diffusive propagation of extragalactic UHECR has been studied already in earlier work. The stationary diffusion from Virgo cluster was considered by Wdowczyk and Wolfendale (1979), Giller et al. (1980) and non-stationary diffusion from a nearby source was studied by Berezinsky et al. (1990a), Blasi and Olinto (1999b) using the the Syrovatsky solution (Syrovatskii (1959)) of the diffusion equation. In this case the GZK cutoff can be absent. A very similar problem was considered again more recently by Isola et al. (2002)).

In this paper we shall study how propagation influences the diffuse energy spectrum of UHECR. We shall prove the theorem that if distance between sources is much smaller than all propagation lengths, the spectrum has the same universal form independent of the mode of propagation. For diffusion in magnetic fields we shall demonstrate how the spectra converge to the universal one when the separation between sources diminishes. Finally, we shall obtain, with the help of the Syrovatsky solution, the spectra for strong magnetic field. In this case with large enough separation between sources, the GZK cutoff becomes weak or absent, and we will discuss the physical explanation of this phenomenon.

## 2. PROPAGATION THEOREM

Let us consider a case when identical UHECR sources are distributed uniformly [1] in the space, with $d$ being the separation between sources. We will demonstrate that if $d$ is less than all other characteristic lengths of propagation, such as diffusion length $l_d(E)$ and energy attenuation length $l_{att}(E)$ given by

$$l_{att} = cE/(dE/dt), \tag{1}$$

then the diffuse energy spectrum has a universal (standard) form *independent of the mode of particle propagation*. In particular, under the conditions specified above the magnetic field, both weak and strong, does not affect the shape of the energy spectrum.

Explicitly, this theorem can be formulated as follows:

*For a uniform distribution of identical sources with separation much less than the characteristic propagation lengths, the diffuse spectrum of UHECR has a universal (standard) form, independent of the mode of propagation.*

First, we shall consider the proof based on the conservation of the number of particles (e.g. protons or nuclei) during the propagation. Let $t$ be the age of the universe with the present age taken as $t_0$. The number of particles per unit volume of the present universe is equal to the number of particles injected into this volume during all history of the universe, independent of the mode of propagation. The homogeneity of particles needed for this statement is provided by almost homogeneous distribution of sources. Thus, the comoving space density of particles $n_p(E)$ from uniformly distributed sources with an age-dependent comoving density $n_s(t)$ and age-dependent generation rate by a source, $Q(E,t)$, is given by

$$n_p(E)dE = \int_0^{t_0} dt Q(E_g,t) n_s(t) dE_g, \tag{2}$$

where $E_g(E,t)$ is the required generation energy at age $t$, if the observed energy is $E$. Eq. (2) does not depend on the way particles propagate.

The homogeneous distribution of particles in presence of inhomogeneous magnetic fields follows from the Liouville theorem and can be explained in the following way. Suppose we have an observer in the space with a magnetic field. The diffuse flux in any direction is given by the integral $\int n_s(l)dl$ over the trajectory of a particle (or antiparticle emitted from the observation point). If $n_s$ is almost homogeneous, the integral depends on the time of propagation and does not depend on the strength and inhomogeneity of magnetic field.

[1] In this paper we shall distinguish between *uniform* and *homogeneous* distribution of the sources: under the latter we assume a continuous and distance-independent distribution.

To find the explicit form of the universal spectrum $n_p(E)$, one needs some additional assumptions. Let us consider the protons as primaries with continuous energy losses due to interaction with the CMB radiation

$$dE/dt = -b(E,t). \tag{3}$$

Here and everywhere below $b(E,t) > 0$. We shall use the connection between the redshift $z$ and cosmological time $t$ according to the standard cosmology

$$dt = \frac{dz}{H_0(1+z)\sqrt{(1+z)^3\Omega_m + \Omega_\Lambda}}, \tag{4}$$

with $H_0, \Omega_m$ and $\Omega_\Lambda$ being the Hubble constant, relative cosmological density of matter and relative density of vacuum energy, respectively.

The generation rate is assumed to be the same for all sources and is taken in the form

$$Q(E,t) = L_p(1+z)^\alpha K(\gamma_g) q_{gen}(E_g) \tag{5}$$

where $L_p$ is the CR luminosity of the source with $(1+z)^\alpha$ describing the possible cosmological evolution of luminosity. The normalization factor $K(\gamma_g)$ is $\gamma_g - 2$ if $\gamma_g > 2$ and $1/\ln(E_{\max}/E_0)$ if $\gamma_g = 2$, with $E_0$ and $E_{\max}$ the minimum and maximum generation energies, respectively. The comoving density $n_s(t)$ of the sources can also contain the evolutionary factor $(1+z)^\beta$, with $\alpha + \beta = m$. Here and everywhere else we assume $E_0 = 1$ GeV, all energies $E$ are measured in GeV and $L_p$ in GeV/s.

Then from Eq. (2) we obtain the normalized universal spectrum as:

$$J_p(E) = \frac{c}{4\pi}\mathcal{L}_0 K(\gamma_g) \int_0^{z_{\max}} dz \left(\frac{dt}{dz}\right)(1+z)^m q_{gen}(E_g)\frac{dE_g}{dE} \tag{6}$$

where $J_p$ is diffuse flux, $\mathcal{L}_0 = L_p n_s$ is the emissivity at $z = 0$, $dt/dz$ is given by Eq. (4), $E_g$ is calculated as $E_g = E_g(E,z)$ and $dE_g/dE$ is given by (Berezinsky and Grigorieva (1998), Berezinsky et al. (2002a))

$$\frac{dE_g(z_g)}{dE} = (1+z_g) exp\left\{\frac{1}{H_0}\int_0^{z_g} dz \frac{(1+z)^2}{\sqrt{\Omega_m(1+z)^3 + \Omega_\Lambda}}\left(\frac{db_0(E')}{dE'}\right)_{E'=(1+z)E_g(z)}\right\}, \tag{7}$$

where $b_0(E)$ is the proton energy loss at $z = 0$.

The generation spectrum $q_{gen}(E_g)$ is not known apriori. Three kinds of spectrum might be considered: (i) the power law spectrum $q_{gen}(E_g) = E_g^{-\gamma_g}$ with $\gamma_g > 2$ and the normalization factor $K(\gamma_g) = \gamma_g - 2$, (ii) the power-law spectrum $q_{gen}(E_g) = 1/E_g^2$ with $K(\gamma_g) = 1/\ln(E_{max}/E_0)$ and (iii) the complex spectrum

$$q_{\rm gen}(E_g) = \begin{cases} 1/E_g^2 & \text{at } E_g \le E_c \\ E_c^{-2}(E_g/E_c)^{-\gamma_g} & \text{at } E_g \ge E_c \end{cases} \tag{8}$$

with

$$K(\gamma_g) = \frac{1}{\ln\frac{E_{max}}{E_c} + \frac{1}{\gamma_g - 2}}.$$

In numerical calculations with the complex spectrum (8) we use $\gamma_g = 2.7$, which gives the best fit to observational data (Berezinsky et al. (2003)).

The universal spectrum (6) with $q_{\rm gen}$ from Eq. (8) and with $m = 0$ is shown in Fig. 1 in comparison with experimental data of AGASA and HiRes arrays. From these figures one can see the good agreement of the universal spectrum with experimental data of both detectors up to $8 \times 10^{19}$ eV. The required emissivities $\mathcal{L}_0$ are: $\mathcal{L}_0 \simeq 1.8 \times 10^{46}$ erg/Mpc$^3$yr and $\mathcal{L}_0 \simeq 8.9 \times 10^{45}$ erg/Mpc$^3$yr for the AGASA and HiRes data, respectively. The excess of AGASA events at $E > 1 \times 10^{20}$ eV needs another component of UHECR.

Under the condition $d << l_{\rm prop}$ the energy spectrum (6) is the same (universal) for rectilinear propagation and propagation in weak and strong magnetic fields. If $l_{\rm prop} \le d$ (or $l_{\rm prop} << d$) the propagation theorem is not valid any more. The distortion of the universal spectrum occurs at $E \ge E_{GZK}$ due to several effects: inhomogeneity of distribution of UHECR sources (local enhancement or local absence of the sources), fluctuation in the distribution of sources, fluctuations of the photopion energy losses over the distance $d$ and due to the small diffusion length $l_d < d$ in case of strong magnetic fields.

## 3. KINETIC EQUATION AND UNIVERSAL SPECTRUM

We have obtained the universal spectrum above from the very general condition of particles conservation during propagation. In this Section we shall demonstrate that the universal spectrum follows also from the kinetic equation.

Let us consider the kinetic equation for a *homogeneous* distribution of the sources (see footnote [1]). Since in this case the particle distribution is also homogeneous, the diffusion term in the kinetic equation is absent, and it has the form:

$$\frac{\partial n_p(E,t)}{\partial t} = \frac{\partial}{\partial E}\left[b(E,t) n_p(E,t)\right] + Q_g(E,t), \tag{9}$$

with $Q_g = n_s Q$. Let us start with a simple stationary equation when $Q_g$, $n_p$ and $b$ do not depend on time:

$$-\frac{\partial}{\partial E}\left[b(E) n_p(E)\right] = Q_g(E) \tag{10}$$

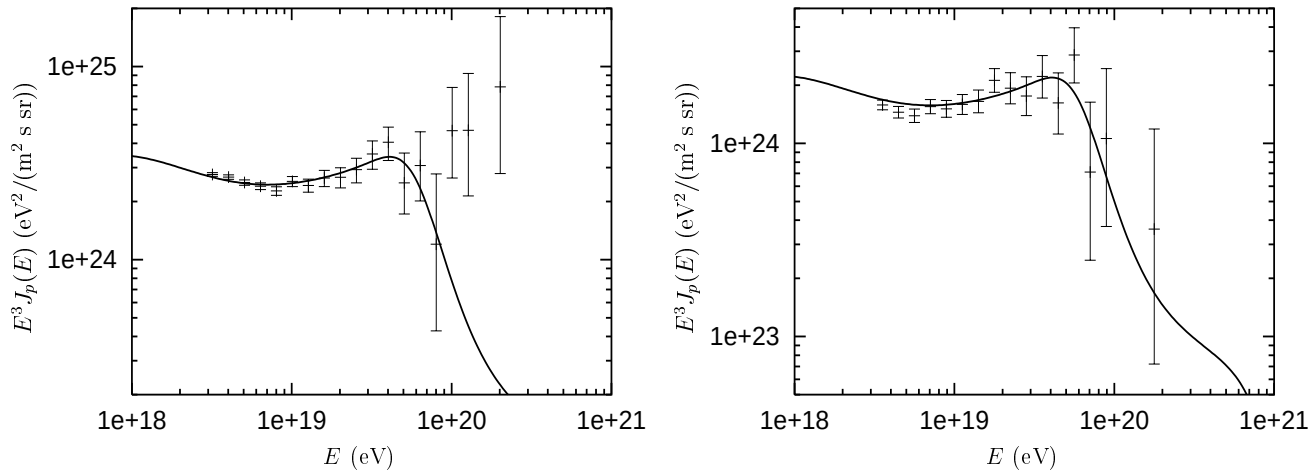


FIG. 1.— Universal spectrum in comparison with the AGASA (left panel) and HiRes data (right panel).

The solution of Eq. (10) is

$$n_p(E) = \frac{1}{b(E)} \int_E^{E_{\max}} dE_g Q_g(E_g) = \int dt \frac{b(E_g)}{b(E)} Q_g(E_g), \tag{11}$$

where $E_g(E,t)$ is the generation energy at time $t$ and we used $dE_g = -b(E_g)dt$. Using $dE = -b(E)dt$ for the same interval $dt$ we obtain $b(E_g)/b(E) = dE_g/dE$ and

$$n_p(E) = \int dt Q_g(E_g(t)) \frac{dE_g}{dE}, \tag{12}$$

in agreement with Eqs. (2) and (6).

Let us now come back to Eq. (9) with time dependent quantities $Q_g, n_p$ and $b$, where $b(t)$ includes also adiabatic energy losses due to redshift. Introducing the new quantities: $\tilde{b}(E,t) = b(E)/H(t)$, $\tilde{Q}_g(E,t) = Q_g(E,t)/H(t)$ and $\tau = (1+z_{max})/(1+z)$, where $z_{max}$ is the maximal redshift in the evolution of sources, we obtain the equation

$$\frac{\partial n_p(E,\tau)}{\partial \tau} = -\frac{\partial \tilde{b}(E,\tau)}{\partial E} n_p(E,\tau) + \tilde{Q}_p(E,\tau). \tag{13}$$

Eq. (13) may be solved with the help of an integration factor

$$\mu(\tau) = \exp\left( -\int_0^\tau d\tau' \frac{\partial \tilde{b}}{\partial E}(\tau') \right) \tag{14}$$

Assuming $n_p(E, z_m) = 0$, we obtain

$$n_p(E,\tau) = \frac{1}{\mu(\tau)} \left[ \int_0^\tau d\tau' \mu(\tau') \tilde{Q}_g(E,\tau') \right]. \tag{15}$$

At this stage the energy losses should be separated into those due to redshift and those due to the interaction with the CMB radiation

$$b(E',z) = E' H_0 \sqrt{\Omega_m (1+z)^3 + \Omega_\Lambda} + (1+z)^2 b_0^{\rm CMB}\left(E'(1+z)\right) \tag{16}$$

where $E'$ is an arbitrary energy at epoch $z$.

Coming back to the variable $z$ in Eq. (13) and inserting there $\partial b(E,z)/\partial E$ from Eq. (16) we obtain after integration

$$n_p(E) = \frac{1}{H_0} \int_0^{z_{max}} \frac{dz}{\sqrt{\Omega_m (1+z)^3 + \Omega_\Lambda}} Q_g(E_g, z) \times$$
$$\times \exp\left[ \frac{1}{H_0} \int_0^z \frac{dz'(1+z')^2}{\sqrt{\Omega_m (1+z')^3 + \Omega_\Lambda}} \left( \frac{\partial b_0(E',z')}{\partial E'} \right)_{E'=(1+z)E_g(z')} \right], \tag{17}$$

which, after introducing the explicit expression for $Q_g$ from Eq. (5), coincides exactly with Eqs. (6) and (7).

## 4. DIFFUSION EQUATION AND THE SYROVASTSKY SOLUTION

In the previous section we have considered the case of a homogeneous distribution of sources, and proved that the universal spectrum is a solution of the kinetic equation (9). We shall now assume a non-homogeneous distribution of the sources. Then one should add the propagation term in Eq. (9). We assume the diffusive propagation in large-scale magnetic fields. For a single source at point $\vec{r}_g$ the diffusion equation has the form:

$$\frac{\partial n_p(E,r)}{\partial t} - \mathrm{div}\left[D(E,r,t)\nabla n_p(E,r)\right] - \frac{\partial}{\partial E}\left[b(E)n_p(E,r)\right] = Q(E,t)\delta(\vec{r}-\vec{r}_g) \tag{18}$$

where $D(E,r,t)$ is the diffusion coefficient that depends on the magnetic field structure. We refer the reader to the Section 5 for a detailed discussion of the relation between the diffusion coefficient and the magnetic field.

In the case when $D$, $b$ and $Q$ depend only on energy, the exact analytic solution of Eq. (18), found by Syrovatskii (1959), is

$$n_p(E,r) = \frac{1}{b(E)}\int_E^\infty dE_g Q(E_g)\frac{exp\left[-\frac{r^2}{4\lambda(E,E_g)}\right]}{\left(4\pi\lambda(E,E_g)\right)^{3/2}}, \tag{19}$$

where

$$\lambda(E,E_g) = \int_E^{E_g} d\epsilon \frac{D(\epsilon)}{b(\epsilon)} \tag{20}$$

is the Syrovatsky variable which has the meaning of the squared distance traversed by a proton in the observer direction, while its energy diminishes from $E_g$ to $E$.

According to the propagation theorem, integrating the Syrovatsky solution over homogeneously distributed sources with density $n_s$,

$$n_p(E) = \int_0^\infty dr 4\pi r^2 \frac{n_s}{b(E)}\int_E^\infty dE_g Q(E_g)\frac{exp\left[-\frac{r^2}{4\lambda(E,E_g)}\right]}{\left(4\pi\lambda(E,E_g)\right)^{3/2}}\ , \tag{21}$$

must result in the universal spectrum. One easily sees this by changing the order of integration in Eq. (21) and using

$$\int_0^\infty dr \frac{4\pi r^2}{\left(4\pi\lambda\right)^{3/2}} exp\left[-\frac{r^2}{4\lambda}\right] = 1\ ,$$

which gives the diffuse space density of protons

$$n_p(E) = \frac{n_s}{b(E)}\int_E^\infty dE_g Q(E_g) \tag{22}$$

in agreement with Eq. (11), where $Q_g(E) = n_s Q(E)$

Coming back to the non-homogeneous case, let us consider a lattice with total size $a$ and UHECR sources located in the lattice vertexes separated by a distance $d$. Using this model for the source distribution, we shall demonstrate the consistency of the Syrovatsky solution with the propagation theorem. We will show that when the separation between sources, $d$, tends to a small value $d_{lim}$, the Syrovatsky solution gives the universal spectrum.

Using the lattice distributed sources and the Syrovatsky solution, one obtains the diffuse flux as

$$J_p(E) = \frac{c}{4\pi}\frac{1}{b(E)}\sum_i \int_E^{E_{max}} dE_g Q(E_g)\frac{exp\left[-\frac{r_i^2}{4\lambda(E,E_g)}\right]}{\left(4\pi\lambda(E,E_g)\right)^{3/2}} \tag{23}$$

where $\lambda(E,E_g)$ is given by Eq. (20) and the summation goes over all sources in the lattice vertexes. The maximum energy in Eq.(23) is given by the smaller of two quantities: the maximum acceleration energy $E_g^{\max}$, and the generation energy $E_g(E,ct_0)$ of a proton with present energy $E$ propagating during a time $t_0$. For the energies $E$ at interest, the former is always smaller that the latter, and we use as $E_{\max}$ the maximum acceleration energy.

We have to specify now the diffusion coefficient $D(E)$, which determines $\lambda(E,E_g)$ in Eq. (23). Putting off the detailed discussion until the Section 5, we will give here a short description of the diffusion coefficients used in this work.

We assume diffusion in a random magnetic field with the mean value $B_0$ on the maximum coherent length $l_c$. This assumption determines the diffusion coefficient $D(E)$ at the highest energies when the proton Larmor radius, $r_L(E) \gg l_c$:

$$D(E) = \frac{1}{3}\frac{c r_L^2(E)}{l_c} \tag{24}$$

At "low" energies, when $r_L(E) \lesssim l_c$ we shall consider three cases:

(i) energy-independent diffusion coefficient

$$D = \frac{1}{3}c l_c, \tag{25}$$

(ii) the Bohm diffusion coefficient, which provides the lowest value of $D$

$$D_B(E) = \frac{1}{3}c r_L(E), \tag{26}$$

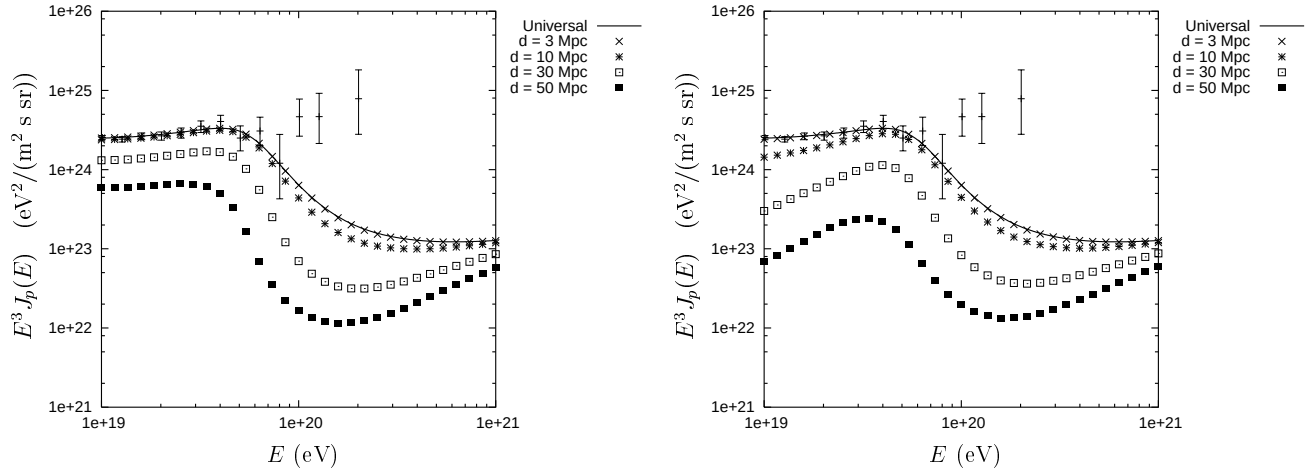


FIG. 2.— Convergence of the diffusion spectrum to the universal spectrum in the case of the Bohm diffusion, $D = D_0(E/E_c)$ at $E < E_c$ (right panel) and in the case of diffusion with $D = D_0$ at $E < E_c$ (left panel). In the calculations the complex generation spectrum (8) has been used. The separations $d$ of the sources are indicated in the figure. The spectra are compared with the AGASA data.

(iii) the Kolmogorov diffusion coefficient

$$D_K(E) = \frac{1}{3} c l_c \left(\frac{r_L(E)}{l_c}\right)^{1/3}. \tag{27}$$

In all three cases we normalized the diffusion coefficients by $(1/3)cl_c$ at $r_L = l_c$ (see Section 5). The characteristic energy $E_c$ of the transition between the high energy and low energy regimes is determined by the condition $r_L(E) = l_c$ and is

$$E_c = 0.93 \times 10^{18} \left(\frac{B_0}{1 \text{ nG}}\right) \left(\frac{l_c}{Mpc}\right) \text{ eV}. \tag{28}$$

One can describe the low-energy and high-energy diffusion regimes with the help of an interpolation formula for the diffusion length:

$$l_d(E) = \Lambda_d + \frac{r_L^2(E)}{l_c} \tag{29}$$

with $\Lambda_d = l_c$ for the regime with $D = const$, $\Lambda_d = r_L(E)$ for the Bohm diffusion and $\Lambda_d = l_c(r_L/l_c)^{1/3}$ for the Kolmogorov regime. For the later use, we shall formalize the description of these three regimes using

$$\Lambda_d(E) = l_c(r_L/l_c)^{\alpha}, \tag{30}$$

with $\alpha$ equal to 0, 1 and 1/3 for the $D = const$, Bohm and Kolmogorov regimes.

For completeness we shall give also the numerical expression for the Larmor radius:

$$r_L(E) = 1.08 \times 10^2 \frac{E}{1 \times 10^{20} \text{ eV}} \frac{1 \text{ nG}}{B} \text{ Mpc}. \tag{31}$$

One can see, therefore, the existence of two different propagation lengths that should be compared with the distance $d$ between sources. These two lengths are $l_{att}$ given by Eq. (1) and $l_d$ given by Eq. (29). The former is large even at the highest energies ($l_{att} \sim 25$ Mpc at $E \sim 10^{21}$ eV) while the latter can be small enough at the energies of interest $10^{19} \leq E \leq 10^{21}$ eV. For a representative case $B_0 = 100$ nG and $l_c = 1$ Mpc we have $l_d(E_c) = l_c = 1$ Mpc at $E_c \approx 1 \times 10^{20}$ eV.

In Fig. 2 we compare the universal spectrum with diffusion spectra characterized by different separations $d$. The diffusion spectra are computed using the diffusion length (29) for the two extreme cases $\Lambda_d = r_L(E)$ and $\Lambda_d = l_c$, both for the representative case $B_0 = 100$ nG and $l_c = 1$ Mpc. Here and below we use for the total lattice size $a = 300$ Mpc, while the control calculations have been performed up to $a = 1000$ Mpc. Increasing $a$ does not change the fluxes. The universal spectrum is calculated with time-independent energy losses, as in the Syrovatsky solution, according to Eq. (6) with $\mathcal{L}_0 = L_p n_s \simeq 2.8 \times 10^{46}$ erg/Mpc$^3$yr.

One can see that in both cases the diffusion spectrum tends to the universal one as the separation $d$ between sources diminishes.

## 5. DIFFUSIVE PROPAGATION

In this section we will study the propagation of UHE particles in the intergalactic turbulent magnetic plasma. Turbulent motion can be considered as random pulsations at different scales, described as an ensemble of many waves with large amplitudes and random phases. The energy is assumed to be injected at the largest scale $l_c$ due to the external processes,

such as the contraction of large-scale structures, large-scale shocks etc, and the scale $l_c$ might be determined by these processes. This scale might coincide with the size of the region filled by the turbulent plasma, in case of small structures. The smallest scale $l_{\min}$ is determined by the dissipation of turbulent motion into thermal energy.

We shall consider *magnetic turbulence* described by the superposition of MHD waves $A\exp[i(-\omega t+\vec{k}\vec{r})]$ with different frequencies $\omega$ and different wave numbers $\vec{k}$. The amplitude $A$ is related to magnetic field $B$, density $\rho$, pressure $P$, velocity $v$ etc. These waves propagate with the Alfven velocity $u_A = B/\sqrt{4\pi\rho}$. The kinetic energy of gas in turbulent motion and the magnetic energy in MHD waves are equal at all scales $\lambda$ (Landau and Lifshitz (1987)):

$$\rho v_\lambda^2 \sim B_\lambda^2/4\pi. \tag{32}$$

For a detailed description of magnetic turbulent plasma and its description as an ensemble of MHD waves we refer the reader to the books: Landau and Lifshitz (1987), Arzimovich and Sagdeev (1979).

For practical calculations of the UHECR propagation, the magnetic field scale spectrum $\langle B^2\rangle_k$ as a function of $k$ is needed. One should clearly distinguish between the magnetic field $\vec{B}_\lambda = \langle\vec{B}\rangle_\lambda$, on the scale $\lambda = 2\pi/k$ and the Fourier component of the field $\vec{B}(k)$ (see Appendix). The physical magnetic field which determines the diffusion of UHE particles is $B_\lambda$.

The turbulence spectrum is described by the dependence of the spectral energy density $w(k)$ on the wave number $k$. It can be expressed using the magnetic energy density $kw(k) \sim B_\lambda^2/8\pi$. Usually the spectra have a power-law form: $w(k) \propto k^{-m}$.

In many practical cases the observations confirm the Kolmogorov (Kolmogorov (1941)) spectrum of turbulence with $m = 5/3$. This spectrum belongs to a class where the initial energy is assumed to be injected at the largest scale $l_c$ and then is transferred to lower scales $l$ in non-linear processes of wave interactions until it dissipates to thermal energy at the lowest scale $l_{\min}$. The Kolmogorov spectrum can be derived assuming that energy flux from one scale to another does not depend on the scale $k$ (Arzimovich and Sagdeev (1979)), i.e.

$$kw(k)/\tau_k = const, \tag{33}$$

where $\tau_k$ is the time for energy transfer to the scale $k$. Since this process is caused by the non-linear term $(v\nabla)v \sim kv^2$ in the Euler equation, one can estimate $\tau_k$ as

$$\tau_k \sim 1/kv_k, \tag{34}$$

where the turbulent velocity can be estimated from equation $kw(k) \sim \rho v_k^2$. Then one immediately obtains $w(k) \propto k^{-5/3}$, i.e. the Kolmogorov spectrum.

Landau and Lifshitz (1987) argue that while scale-independent energy flux is a reasonable assumption in ordinary hydrodynamics, for MHD waves it is proportional to $v_k^4$. In this case one obtains the Kraichnan (1965) spectrum $w(k) \propto k^{-3/2}$.

In the case of shock waves, the spectrum is (Vainstein et al (1989)) $w(k) \propto k^2$.

### 5.1. *Diffusion coefficient for UHE protons*

Now we shall proceed with calculations of the diffusion coefficient $D(E)$ for UHE protons in extragalactic magnetic fields, which are characterized by the spectrum of turbulence $w(k) \propto k^{-m}$, with the basic scale $l_c$ and with the magnetic field on this scale $B_0$. We shall use the characteristic energy $E_c$, defined by Eq. (28) from the condition $r_L(E_c) = l_c$, where the Larmor radius $r_L$ is given by Eq. (31).

First we obtain the asymptotic expression for $D(E)$ valid when $r_L \gg l_c$, i.e. at $E \gg E_c$. The diffusion length $l_d$ is determined as the distance at which the average angle of scattering satisfies

$$\langle\theta^2\rangle \sim n\left(\frac{l_c}{r_L}\right)^2 \sim 1,$$

where the number of scatterings $n$ is given by $n \sim l_d/l_c$. It results in the diffusion length $l_d(E) \approx r_L^2/l_c$, and thus the diffusion coefficient, $D(E) = (1/3)cl_d(E)$, in the asymptotic limit $r_L \gg l_c$ is given by

$$D_{\rm asymp}(E) = 3.6\times10^{34}E_{20}^2\left(\frac{100\ {\rm nG}}{B_0}\right)^2\left(\frac{1\ {\rm Mpc}}{l_c}\right)\ {\rm cm}^2/{\rm s}. \tag{35}$$

We shall calculate now the diffusion coefficient in the low-energy limit $r_L \ll l_c$ (i.e. at $E \ll E_c$). We will follow the V. Ptuskin method given in Chapter 9 of the book Berezinsky et al. (1990b). Let us consider the scattering of UHE protons with $r_L \ll l_c$ in a magnetic field of MHD wave $B_\lambda\exp[i(\vec{k}\vec{r}-\omega t)]$. The magnetic field on the basic scale $\vec{B}_0$ is considered as constant field for smaller scales $\lambda$.

Scattering of UHE protons off the MHD waves in the regime $r_L \ll l_c$ is dominated by resonance scattering (see Lifshitz and Pitaevskii (2001), Sections 55 and 61). The condition for resonant scattering is given by $\omega' = s\omega'_B$, where $\omega'$ and $\omega'_B = eB/\gamma' mc$ are the wave frequency and the giro-frequency in the system $K'$ at rest with particle motion along the field $\vec{B}_0$, and $s = 0,\ \pm1,\ \pm2$.... After a Lorentz transformation to the laboratory system, one obtains

$$\omega - k_\parallel v_z = s\omega_B, \tag{36}$$

where $\omega$ is the wave frequency, $k_\parallel$ is the projection of the wave vector onto the direction of $\vec{B}_0$ , $v_z$ is the projection of particle velocity onto the same direction, and $\omega_B = eB/\gamma mc$. For a magnetized plasma $r_L \ll \lambda_\perp$ (or equivalently $k_\perp v_\perp/\omega_B \ll 1$) and $s = \pm 1$ (Berezinsky et al. (1990b)). Thus from Eq. (36) one derives the resonant wave number

$$k_\parallel^{\rm res} = \left| \frac{\omega(k) \pm \omega_B}{v_z} \right| \approx \frac{\omega_B}{v\mu} = \frac{1}{r_L \mu}, \tag{37}$$

where $\mu = \cos\theta$ and $r_L = v/\omega_B$ is the Larmor radius. In deriving Eq. (37) we have used $\omega(k) \ll \omega_B$, which follows from the dispersion relation for Alfven waves $\omega(k) = u_A k_\parallel$ (Landau and Lifshitz (1987)), and $v/u_A \gg 1$ for ultrarelativistic particles.

We shall assume here first the Kolmogorov spectrum normalized at the basic scale $k_0 = 2\pi/\lambda_0$:

$$kw(k) = k_0 w_0 (k/k_0)^{-2/3}, \tag{38}$$

where $w(k)$ is the spectral magnetic energy density normalized as $k_0 w_0 = B_0^2/8\pi$.

We shall adopt from Berezinsky et al. (1990b) (chapter 9) the diffusion coefficient $D_\parallel$ (in the direction of $\vec{B}_0$) expressed with the frequencies of particle scattering off the waves:

$$\nu(\mu, k_{\rm res}) = \frac{1}{2}(\nu^+ + \nu^-) = 2\pi^2 \omega_B k_{\rm res} \omega(k_{\rm res})/B_0^2$$

$$D = \frac{v^2}{4} \int_0^1 d\mu \frac{1-\mu^2}{\nu(\mu, k)}, \tag{39}$$

where $\nu^+$ and $\nu^-$ correspond to waves propagating along the field and in the opposite direction, respectively. From now on the subscript $\parallel$ will be omitted.

Using the formulae above, and performing integration over $\mu$ we obtain

$$D(E) = \frac{18}{7\pi(2\pi)^{2/3}} v l_c \left(\frac{r_L}{l_c}\right)^{1/3}. \tag{40}$$

Numerically

$$D(E) = 2.3 \times 10^{34} E_{20}^{1/3} \left(\frac{100 \text{ nG}}{B_0}\right)^{1/3} \left(\frac{l_c}{1 \text{ Mpc}}\right)^{2/3} \text{ cm}^2/\text{s}. \tag{41}$$

$D(E)$ from Eq. (41) and from Eq. (35) match together fairly well: at energy $E_c$ they differ by 40%.

The calculations for other spectra are similar: in case of the Kraichnan spectrum $w(k) \propto k^{-3/2}$, one obtains $D(E) \propto E^{1/2}$, and for diffusion on shock waves, $w(k) \propto k^{-2}$, $D = const$ follows.

*Diffusion coefficient for static magnetic field.*
This case can be considered as scattering off MHD waves in the limit $\omega(k) \to 0$. Assuming the spectrum

$$kw(k) = \frac{B_0^2}{8\pi} \left(\frac{k}{k_0}\right)^{-\alpha},$$

with $\alpha < 1$ for convergence of the integral, we obtain, performing the same calculations as above:

$$D(E) = \frac{2(2\pi)^{-\alpha}}{\pi(1-\alpha)(3-\alpha)} l_c v \left(\frac{r_L}{l_c}\right)^{1-\alpha}. \tag{42}$$

### 5.2. *Intergalactic medium and formation of turbulent spectrum*

The intergalactic medium is represented by different structures (clusters of galaxies, superclusters, filaments and voids), where the medium properties are very much different. In the estimates below we shall normalize all quantities by the baryon density $n_b = 2.75 \times 10^{-7}$ cm$^{-3}$, corresponding to $\Omega_b = 0.044$ from WMAP measurements (Spergel et al. (2003)), and by the temperature $T \sim 10^6$ K (see e.g. the simulation of Davé et al. (2001) for filaments). Hence, we adopt the sound speed

$$c_s = (\gamma T/m_H)^{1/2} = 1.2 \times 10^7 (T/10^6)^{1/2} \text{cm/s}, \tag{43}$$

the Alfven velocity

$$u_A = \frac{B}{\sqrt{4\pi\rho_b}} = 4.2 \times 10^5 \frac{B}{1 \text{ nG}} \left(\frac{2.75 \times 10^{-7} \text{ cm}^{-3}}{n_b}\right)^{1/2} \text{ cm/s}, \tag{44}$$

and the Coulomb scattering length for electron-electron and proton-proton scattering

$$l_{\rm sc} = \frac{T^2}{4\pi e^4 n_b L} = 1.7 \left(\frac{T}{10^6}\right)^2 \frac{2.75 \times 10^{-7}}{n_b} \text{ kpc}, \tag{45}$$

where $L \sim 20$ is the Coulomb logarithm. The short scattering length $l_{\rm sc}$ in comparison with the basic scale $l_c$ is one of the conditions which are needed to provide the turbulent regime.

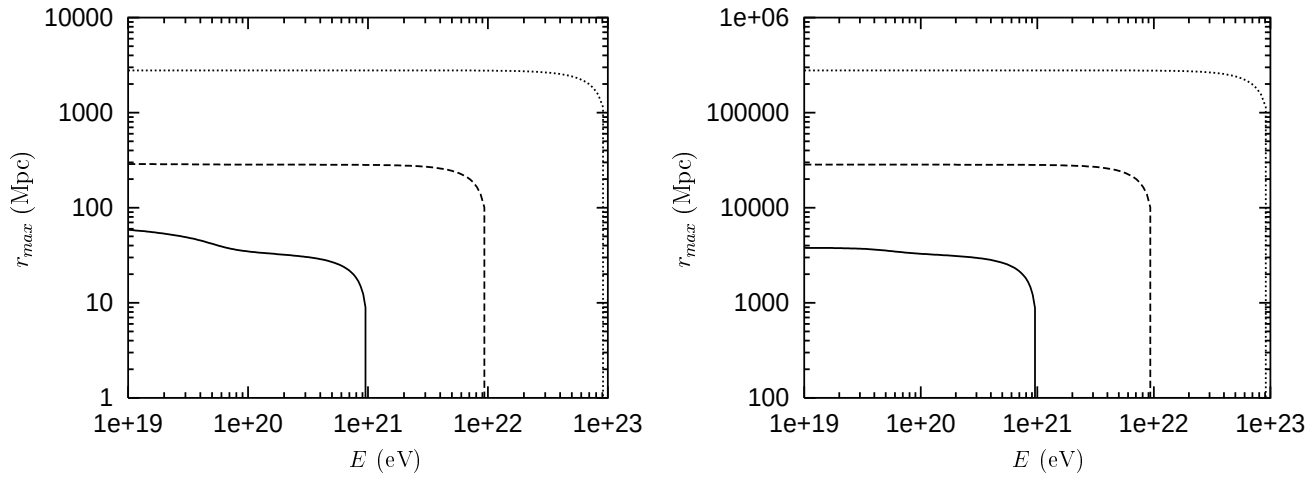


FIG. 3.— Maximum distance to a source $r_{\max}(E) = 2\sqrt{\lambda(E, E_g^{\max})}$ for diffusive propagation. Continous line: $E_g^{\max} = 1 \times 10^{21}$ eV, dashed line: $E_g^{\max} = 1 \times 10^{22}$ eV, dotted line: $E_g^{\max} = 10^{23}$ eV. Magnetic field configuration is $(B_0, l_c) =$ (100 nG, 1 Mpc) (left panel) and $(B_0, l_c) =$ (1 nG, 1 Mpc) (right panel).

With the characteristics of the media above, we shall discuss now, whether the equilibrium turbulence spectrum in the gas can be formed during the age of the universe $t_0$. We shall make estimates for the Kolmogorov spectrum.

The relaxation time $\tau_k$ to the equilibrium Kolmogorov spectrum is given by Eq. (34) as $\tau_k \sim 1/kv_k$, where $v_k$ is the turbulent velocity on the scale $k$. Taking $v_k$ from $\rho v_k^2 \sim 2kw(k)$, and using the Kolmogorov spectrum normalized at the basic scale as in Eq. (38), we obtain

$$\tau_k = \frac{1}{k_0}\left(\frac{\rho}{2k_0 w_0}\right)^{1/2}\left(\frac{k}{k_0}\right)^{-2/3}. \tag{46}$$

The longest time is needed for the formation of the spectrum at the largest scale $k_0$:

$$\tau_0 = \frac{1}{k_0}\left(\frac{\rho}{2k_0 w_0}\right)^{1/2}. \tag{47}$$

Using $k_0 w_0 = B_0^2/8\pi$ and $v_0 = B_0/\sqrt{4\pi\rho} = u_A$, we obtain

$$\tau_0 \sim l_c/u_A. \tag{48}$$

Numerically it gives

$$\tau_0 = 2.4 \times 10^{11} \frac{l_c}{1\ \mathrm{Mpc}} \frac{1\ \mathrm{nG}}{B_0}\left(\frac{n_b}{2.75 \times 10^{-7}}\right)^{1/2}\ \mathrm{yr}. \tag{49}$$

Another estimate of the relaxation time $\tau_0$ can be obtained for the sonic turbulence with the Kolmogorov spectrum. The shortest time is given by $\tau_0 = l_c/c_s$, which for a turbulent plasma is the analogue of the causality condition. Numerically it gives

$$\tau_0 = 0.84 \times 10^{10} \frac{l_c}{1\ \mathrm{Mpc}}\left(\frac{10^6\ K}{T}\right)^{1/2}\ \mathrm{yr}. \tag{50}$$

For a more accurate estimate one can use the relaxation time for the sonic turbulence from Arzimovich and Sagdeev (1979)

$$\tau_k \sim \frac{n_b T}{k w_k}\frac{1}{\omega_k}. \tag{51}$$

Using the dispersion relation $\omega_k = k(T/m)^{1/2}$ and the Kolmogorov spectrum $kw_k = k_0 w_0 (k/k_0)^{-2/3}$, with $k_0 w_0 \sim nT$, we obtain numerically an estimate close to that given by Eq. (50).

From the above estimates we can conclude that the Kolmogorov spectrum cannot be reached for MHD turbulence in the voids, where the magnetic field is presumably small, $B_0 \leq 1$ nG. However, it can be established in filaments (see Eq.(49)) in case $B_0 > 1$ nG and $l_c \leq 1$ Mpc, and it has enough time to be developed in galaxy clusters, where the magnetic field is strong and density of gas is larger than in other structures. For other types of turbulence, e.g. for sonic turbulence, these conditions can be somewhat relaxed.

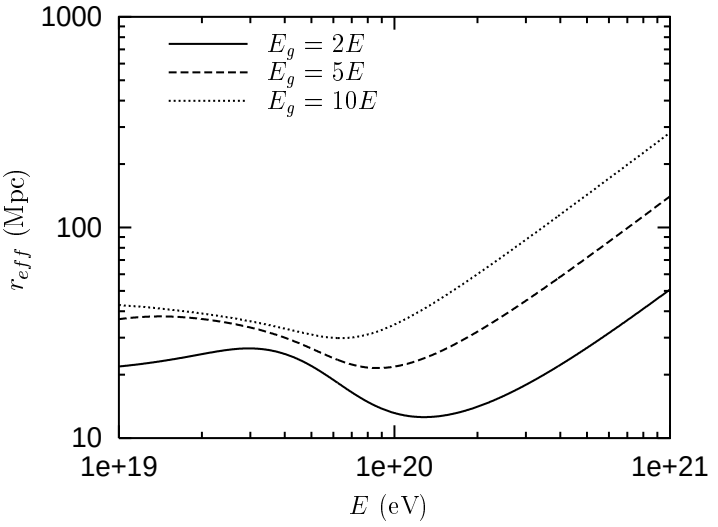


FIG. 4.— Effective distance to a source $r_{eff}(E) = 2\sqrt{\lambda(E, E_g/E)}$ with magnetic field configuration $(B_0, l_c) = (100\ \text{nG},\ 1\ \text{Mpc})$.

### 5.3. *Some features of diffusive propagation*

Inspired by numerical simulations (Yoshiguchi et al. (2003)) we study the diffusion in various magnetic field configurations with the basic parameters $(B_0, l_c)$ in the intervals $B_0 = 10 - 1000$ nG and $l_c = 1 - 10$ Mpc. As a representative configuration we consider (100 nG, 1 Mpc) with $E_c \approx 1 \times 10^{20}$ eV.

The calculated diffuse energy spectra are characterized by the sets $(B_0, l_c, d)$, where $d$ is the separation between sources. We shall use the following definitions. The case when at all relevant (observed) energies $d > l_d(E)$ (or $d \gg l_d(E)$) we shall refer to as *diffusion in a strong magnetic field*. The case when $d \lesssim l_d(E)$ corresponds to *diffusion in a weak magnetic field*.[2] The extreme case $d \ll l_d(E)$ results in the universal spectrum.

*Minimal distance to a source.*

For the diffusion approximation to be valid, a source must be at a distance $r > r_{\min}(E)$. In principle, velocity of light does not enter the diffusion equation, but this equation is not valid when the propagation velocity exceeds the light speed $c$. The value of $r_{\min}(E)$ can be estimated from the condition that the diffusive propagation time must be longer than the time of rectilinear propagation,

$$t_{\text{prop}} \sim \frac{r^2}{D(E)} > \frac{r}{c},$$

as

$$r_{\min}(E) \sim \frac{1}{3} l_d(E). \tag{52}$$

For a source at distance $r \leq r_{\min}(E)$ the protons with energy $E$ or higher propagate in a quasi-rectilinear regime. At $E \geq E_c$ one has

$$r_{\min}(E) = \frac{1}{3} \left(\frac{E}{E_c}\right)^2 l_c.$$

*Maximal distance to a source.*

As seen from Eq. (19) the contribution of a source to the flux at energy $E$ becomes negligible at distances $r > r_{\max}(E)$ with

$$r_{\max}(E) = 2\sqrt{\lambda(E, E_g^{\max})}, \tag{53}$$

where $E_g^{\max}$ is the maximum generation energy provided by a source.

For the representative case $(B_0, l_c) = (100\ \text{nG}, 1\ \text{Mpc})$, $r_{max}$ is plotted in Fig. 3 as a function of $E$ for different values of $E_g^{max}$. One can see that in the case of diffusive propagation only nearby sources contribute the UHECR flux.

In Fig. 4 we have plotted also

$$r_{\text{eff}}(E) = 2\sqrt{\lambda(E, E_g/E)}$$

for different (fixed) ratios $E_g/E = 2, 5$ and 10. The increase of $r_{\text{eff}}$ with $E$ provides the increase of diffuse flux $J_p(E)$ with energy when the distance between sources $d$ is large enough (see Fig. 2).

[2] Note, that this definition does not guarantee the (quasi)rectilinear propagation of particles.

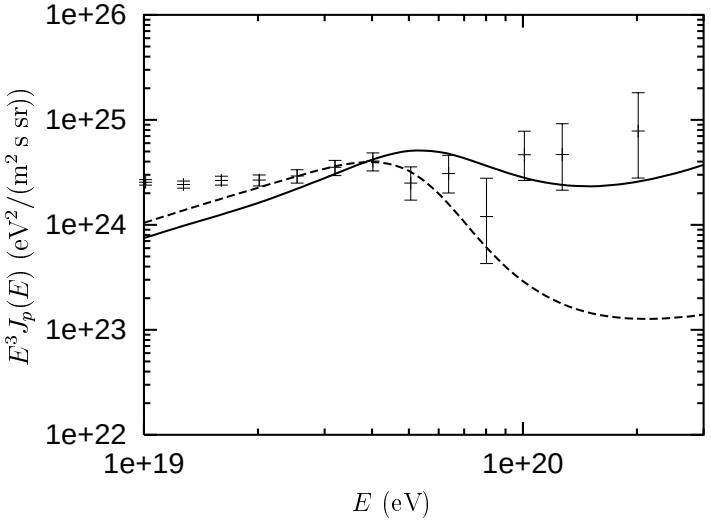


FIG. 5.— Diffusion spectra for two different configurations ($B_0,\ l_c,\ d$). Dashed line corresponds to (100 nG, 1 Mpc, 30 Mpc) with source luminosity $L_p = 8.5\times10^{43}$ erg/s, while continuous line is shown for the same $d$ but for much stronger magnetic field: (1000 nG, 1 Mpc, 30 Mpc), with source luminosity $L_p = 1.5\times10^{47}$ erg/s. In the latter case the GZK cutoff is weak. The spectra are compared with the AGASA data.

## 6. DIFFUSE FLUXES IN THE DIFFUSION APPROXIMATION

In this Section we will compute the diffuse flux according to Eq. (23) as the sum of fluxes from single sources located in the lattice vertexes with a separation $d$ and with a total size $a$. We will assume the complex generation spectrum given by Eq. (8). For the diffusion coefficient we use $D(E) = (1/3)cl_d(E)$ with $l_d(E)$ given by the interpolation formula (29) for the case of Bohm diffusion at $E < E_c$.

At small distances $r \leq r_{\min}(E)$, given by Eq. (52), the fluxes from the individual sources are calculated in the rectilinear approximation, and the diffuse flux is given by

$$J_p^{\rm rect}(E) = \frac{L_p K(\gamma_g)}{4\pi} \sum_i \frac{q_{gen}(E_g(E,r_i))}{r_i^2} \frac{dE_g(E,r)}{dE} \tag{54}$$

At large distances $r \geq r_{\min}(E)$ the diffuse flux is given by Eq. (23), and with explicit normalization has the form

$$J_p^{diff}(E) = \frac{c}{4\pi} \frac{L_p K(\gamma_g)}{b(E)} \sum_i \int_E^{E_{max}} dE_g q_{gen}(E_g) \frac{exp\left[-\frac{r_i^2}{4\lambda(E,E_g)}\right]}{(4\pi\lambda(E,E_g))^{3/2}}, \tag{55}$$

where $E_{max}$ is the maximum acceleration energy (see Section 4). The calculated spectra are presented in Fig. 5.

In Fig. 5 the diffuse spectra are shown for the complex generation spectrum (8) and for two sets of $(B_0, l_c, d)$ equal to (100 nG, 1 Mpc, 30 Mpc), shown by dashed curve, and (1000 nG, 1 Mpc, 30 Mpc), shown by solid curve. Both of them are characterized by the same $d = 30$ Mpc, but in the latter case the magnetic field is much stronger. This case is characterized by $d \gg l_d(E)$ at all observable energies, and hence corresponds to diffusion in the strong magnetic field (see Section 5). From Fig. 5 one can observe that GZK cutoff is weak in this case.

The dashed curve in Fig. 5 is characterized by $l_d(E) = 1(E/E_c)^2$ Mpc at $E > E_c = 1\times10^{20}$ eV, and this regime of propagation can be described as an intermediate one between that for strong and weak magnetic fields.

The regime with weak GZK cutoff (propagation in a strong magnetic field) requires a much higher luminosity $L_p$ to fit the observational data, $L_p = 1.5\times10^{47}$ erg/s, while the intermediate case (100 nG, 1 Mpc, 30 Mpc) needs only $L_p = 8.5\times10^{43}$ erg/s.

We shall analyze now the regime of propagation in strong magnetic field in more detail. First we will comment qualitatively why in the diffusion approximation the GZK cutoff in the spectrum might be weak or absent.

The essence of the GZK cutoff consists of much different energy losses above and below $3\times10^{19}$ eV. Consider, for example, two protons with energies $1\times10^{19}$ eV and $1\times10^{20}$ eV, both propagating rectilinearly from a remote single source. The first proton looses little energy: the ratio $E_g/E$ (with $E_g$ being the generation energy) is not large, and the flux of these protons is weakly suppressed by the generation spectrum. The energy losses of the second proton are large, $E_g/E$ is very high and the flux suppression is dramatic (the GZK cutoff). Now consider the diffusive propagation. A proton with energy $1\times10^{19}$ eV, because of the $D(E)$ dependence, travels much longer time than a proton with $1\times10^{20}$ eV, and it results in increased ratio $E_g/E$, making this ratio comparable with that for the second proton. It causes a less steep GZK cutoff, or its absence. However, the price for the absence of the GZK cutoff is a very high luminosity of the sources $L_p$, needed to provide the observed flux at $E \gtrsim 1\times10^{19}$ eV, e.g. $L_p \gtrsim 1\times10^{47}$ erg/s for the spectrum shown in Fig. 5.

Let us now come over to the quantitative analysis of absence of the GZK cutoff in the strong magnetic fields. Consider the three cases of diffusion regimes at $E < E_c$ with $\alpha = 0,\ 1/3,\ 1$, i.e. $D = const$, Kolmogorov and Bohm regimes,

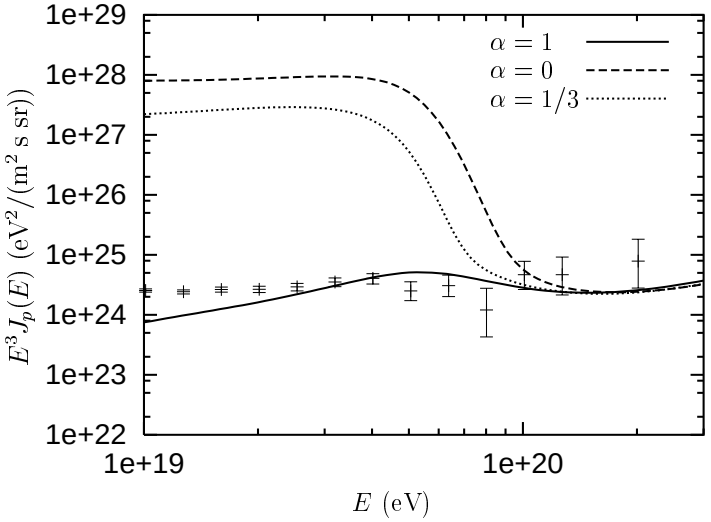


FIG. 6.— Diffuse fluxes from lattice-distributed sources with $d = 30$ Mpc and for magnetic configuration (1000 nG, 1 Mpc). The cases $\alpha = 0,\ 1/3,\ 1$ correspond to $D = const$, Kolmogorov and Bohm diffusion, respectively at $E < E_c \approx 1 \times 10^{21}$ eV. Luminosity of a source is $L_p = 1.5 \times 10^{47}$ erg/s.

respectively (see Eq. (30)). The diffuse spectra calculated for configuration (1000 nG, 1 Mpc, 30 Mpc) are displayed in Fig. 6

Why the three spectra are so much different at low energies and are the same at high energies?

The quantitative explanation can be given explicitly in terms of $\lambda(E, E_g)$, which is the basic parameter of the Syrovatsky solution (see Eq. (19)).

In Fig. 7 we plot the values of

$$r_{\max}(E, E_g) = 2\sqrt{\lambda(E, E_g)},$$

which according to Eq. (19) determines the maximum distance to a source in case the observed energy is $E$ and generation energy is $E_g$. The left panel of Fig. 7 corresponds to $D = const$, the right panel – to the Bohm diffusion.

From Fig. 7 one can see that in the energy interval $(1 - 4) \times 10^{19}$ eV $\quad \lambda(E, E_g)$ practically does not depend on $E_g$. Then from Eq. (19) one obtains for a single source

$$n_p(r, E) = \frac{1}{(\gamma_g - 1)(4\pi)^{3/2}} \frac{Q(E)}{(\lambda(E))^{3/2}\beta(E)} \exp\left(-\frac{r^2}{4\lambda(E)}\right), \tag{56}$$

where $\beta(E) = E^{-1}dE/dt$.

From Eq. (56) and values of $\lambda(E)$ for the two diffusion regimes, one may observe the main effect : strong suppression of flux from nearby sources ($r \sim d \sim 30$ Mpc) in case of the Bohm diffusion and weak suppression in case of $D = const$ diffusion. It occurs because the Bohm diffusion coefficient, $D_B(E) = D_0(E/E_c)$, is small at $E \ll E_c$, and hence $\lambda(E)$ is also small, which results in exponential suppression of the flux, according to Eq. (56). In case $D(E) = D_0$, diffusion coefficient is large, $\lambda(E)$ is large too (see left panel of Fig. 7), and exponential suppression in Eq. (56) is much smaller. This quantitative explanation agrees with the qualitative one, given above: large propagation time, i.e. small diffusion coefficient or small $\lambda$, suppresses the the flux at $E < E_{\rm GZK}$ to the level of the flux at the highest energies.

Let us come over to the higher energies.

One can see from Fig. 7 that at $E \geq 1 \times 10^{20}$ eV for $D = const$ diffusion and $E \geq 1 \times 10^{19}$ eV for the Bohm diffusion $\lambda(E)$ is small but increases fast with energy up to $r_{\max}(E, E_g) \sim 30$ Mpc at $E = E_{\max}$. The exponent in Eq. (19) grows very fast and all other quantities can be taken out of integral at energy $E_g = E_{\max}$. After integration one arrives at analytic expression

$$n_p(r, E) = \frac{Q(E_{\max})}{4\pi r^2} \frac{\sqrt{\lambda_0}}{D_0} \exp - \frac{r^2}{4\lambda_0} \frac{2}{\sqrt{\pi}} \left(\frac{E_{\max}}{E} \frac{\beta(E_{\max})}{\beta(E)}\right) \left(\frac{E_c}{E_{\max}}\right)^2, \tag{57}$$

where $\beta(E) = E^{-1}dE/dt$ and $\lambda_0 = \lambda(E, E_{\max})$, which in fact does not depend on $E$. From Eq. (57) one can see that $n_p(r, E)$ has universal dependence for all diffusion regimes, provided by $D(E_{\max}) = D_0(E_{\max}/E_c)^2$ for all of them. In asymptotically high energy regime (not seen in Fig. 6) $E^3 n_p(E) \propto E^2$.

We found and analysed above the diffusion regime with weak GZK cutoff for very strong magnetic field $B_0 = 1000$ nG. Can this effect exist for much weaker magnetic field? We have not found such regimes in any realistic cases we studied.

The strong restriction to existence of these regimes is imposed by upper limit to the distance between sources $d$. This distance cannot be taken arbitrary large. They are limited by maximum acceleration energy $E_{\max}$, which we keep here reasonably high $E_{\max} = 1 \times 10^{22}$ eV. For rectilinear propagation from a source at distance $r$ the proton with observed

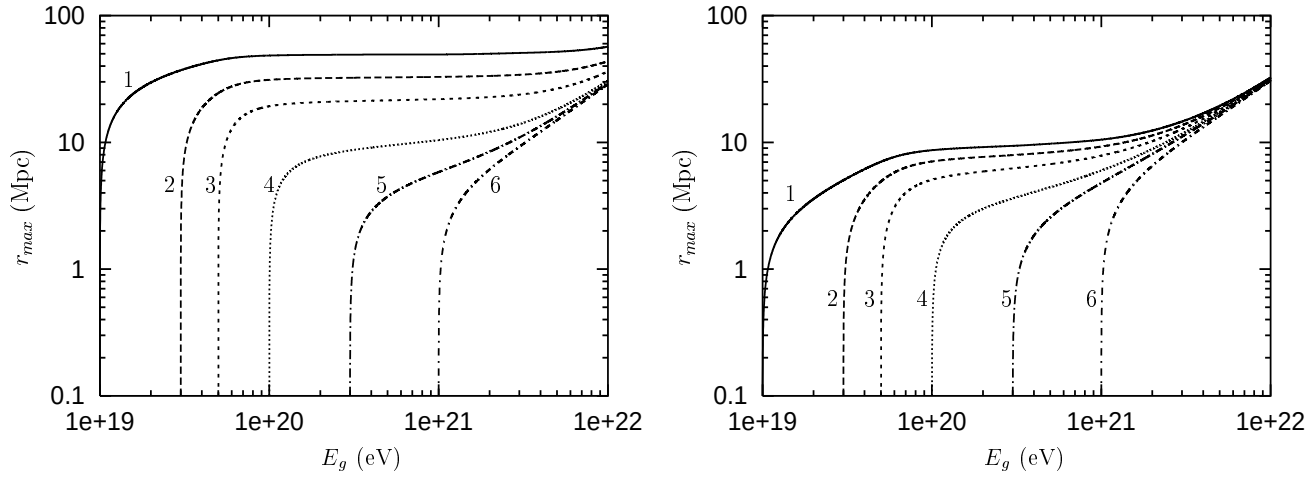


FIG. 7.— The values of $r_{\max}(E, E_g) = 2\sqrt{\lambda(E, E_g)}$ as function of generation energy $E_g$ for the $D = const$ diffusion (left panel) and the Bohm diffusion (right panel). The magnetic field configuration is (1000 nG, 1 Mpc, 30 Mpc). The observed energies E are $1 \times 10^{19}$ eV - curve 1, $3 \times 10^{19}$ eV - curve 2, $5 \times 10^{19}$ eV - curve 3, $1 \times 10^{20}$ eV - curve 4, $3 \times 10^{20}$ eV -curve 5, $1 \times 10^{21}$ eV - curve 6.

energy $E = 1 \times 10^{20}$ eV must have at $r = 100$ Mpc the generation energy $E_g = 1 \times 10^{22}$ eV, and thus the sharp cutoff at $E = 1 \times 10^{20}$ eV is predicted. For $r = 50$ Mpc the cutoff energy energy is $E = 3 \times 10^{20}$ eV. Assuming $r \sim d$, one obtains $d \lesssim 50 - 100$ Mpc for $E_{\max} = 1 \times 10^{22}$ eV.

We have performed many calculations with magnetic fields in the range 100 - 300 nG, with $l_c$ in a range 1 - 10 Mpc, for all three difusion regimes $\alpha = 1,\ 1/3,\ 0$ and with $d$ in a range 30 - 50 Mpc. In all cases the spectra expose GZK cutoff.

On this basis we conclude that in case $E_{\max} \leq 1 \times 10^{22}$ eV, i.e. for $d \lesssim 50$ Mpc, the *diffusion regime* with weak GZK cutoff appears only at very strong magnetic fields $B_0 \sim 1000$ nG, and it needs very high source luminosities $L_p \sim 10^{47}$ erg/s.

## 7. CONCLUSIONS

We have performed a formal study of the propagation of UHE particles, using an analytic approach. We demonstrated that the distance between sources is a crucial parameter which strongly affects the diffuse energy spectrum.

We have proved that, for a uniform distribution of sources, when the separation between them is much smaller than all characteristic propagation lengths, most notably the diffusion length $l_d(E)$ and the energy attenuation length $l_{\rm att}(E)$, the diffuse spectrum of UHECR has a *universal* form, independent of the mode of propagation. This statement has the status of a theorem and is valid for propagation in strong magnetic fields. The proof is given using particle number conservation during propagation and also using the kinetic equation for the propagation of UHE particles. In particular the exact solution to the kinetic equation (9) for a *homogeneous* (*i.e.* continuous and distance-independent) distribution of the sources gives exactly the same spectrum as in the method using particle-number conservation. Note that in Eq.(9) the diffusion term is absent due to homogeneous distribution of the sources.

Another proof of the theorem is given using the diffusion equation (18), and its exact solution (Syrovatskii (1959)) for a single source in the case of time-independent energy losses. We calculated the diffuse flux putting the sources at the vertexes of a big lattice with size $a$ and with separation $d$ between vertexes (sources). The results of the calculations are shown in Fig. 2. One can see that when the distance between sources diminishes from 50 Mpc to 10 Mpc, the spectra converge to the universal spectrum (full curves) and at $d = 3$ Mpc they become identical to the universal spectrum. This result is confirmed by analytic calculations. When the separation between sources is small, summation over the sources can be replaced by an integration and the corresponding spectrum (21) coincides exactly with the universal spectrum.

In this paper we have studied the diffusive propagation of UHE particles in intergalactic space, which is considered as a turbulent magnetic plasma with baryonic gas density $n_b$ and temperature $T$, and with two basic turbulence scales $l_c$, where external energy is injected, and $l_{\min}$, where turbulent energy is dissipated. Turbulent motion is considered to be random pulsations at different scales, described by an ensemble of magneto-hydrodynamic (MHD) waves $B_\lambda \exp[i(-\omega t + \vec{k}\vec{r})]$ with different frequencies $\omega$ and different wave numbers $\vec{k}$. Diffusion arises due to resonant scattering of particles in magnetic fields of MHD waves. At "low" energies, when the Larmor radius $r_L$ is much smaller than the basic scale $l_c$, the diffusion coefficient can be calculated, provided the spectral energy density of the turbulent plasma, $w(k)$, is known as a function of $k$. Such calculations for the Kolmogorov spectrum of turbulence result in the diffusion coefficient given by Eq.(41).

It is interesting to note, that the diffusion in static magnetic fields can be calculated by this method as the limiting case, when wave frequency $\omega \to 0$. The diffusion coefficient for static magnetic fields is given by Eq.(42).

The diffusion coefficient in the high energy limit, when $r_L \gg l_c$, can be reliably calculated as the process of multiple scattering. The diffusion coefficient for this extreme case is given by Eq.(35). The diffusion coefficients in the low energy regime ($r_L \ll l_c$), given by Eq.(41), and in the high energy regime ($r_L \gg l_c$), given by Eq.(35), match each other well.

In practical calculations of the diffuse fluxes we characterize the magnetic configuration by three parameters ($B_0,\ l_c,\ d$),

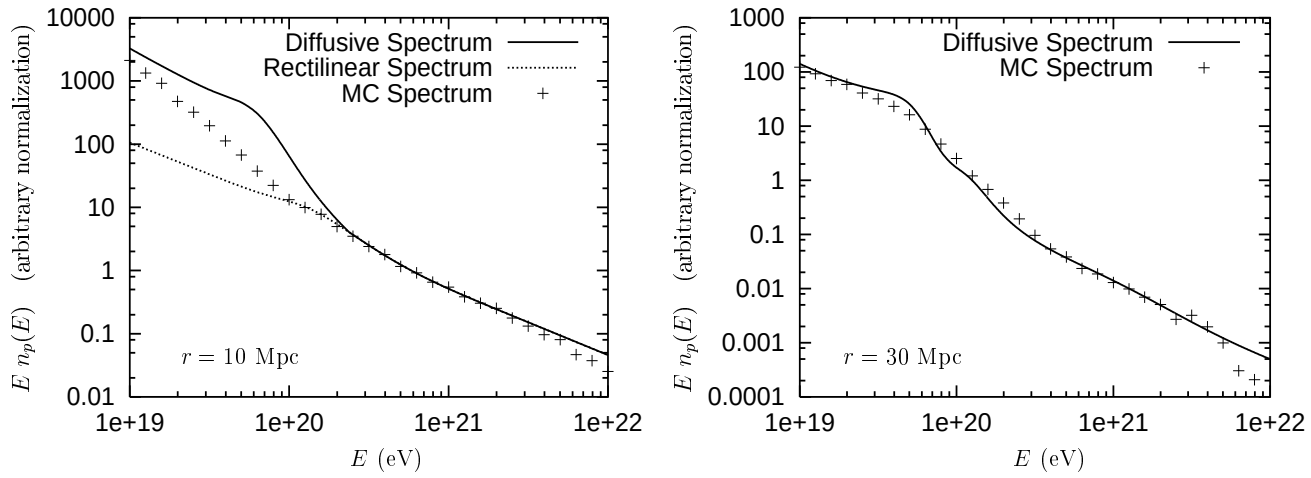


FIG. 8.— Comparison of the analytic diffusive spectrum with the Monte Carlo simulation by Yoshiguchi et al. (2003). The spectra are given in the case of Kolmogorov diffusion with $(B_0, l_c) = (100\ \mathrm{nG}, 1\ \mathrm{Mpc})$ and for a single source placed at distance 10 Mpc (left panel) and 30 Mpc (right panel).

where $B_0$ is the mean magnetic field on the basic scale $l_c$ and $d$ is the separation of sources. We put the sources at the vertexes of a lattice of total size $a$, for which we typically used $a = 300$ Mpc. Increasing $a$ does not change the fluxes. The fluxes from the individual sources were found as the Syrovatsky solution (19), and the diffuse flux was found by summation over all sources, given by Eq.(23). As a representative case for a strong magnetic field, we considered the configuration $(B_0,\ l_c)$=(100 nG, 1 Mpc).

An important feature of the diffusion model is that the observed diffuse flux is produced by nearby sources (see Fig. 3 and 4). The maximum distance $r_{\max}$ depends strongly on the maximum acceleration energy $E_{\max}$. For example, for $E_{\max} = 1{\times}10^{21}$ eV and $(B_0, l_c) = (100\ \mathrm{nG}, 1\ \mathrm{Mpc})$, the maximum distance is less than 70 Mpc, while for $E_{\max} = 1{\times}10^{22}$ eV this distance is 200 Mpc. For smaller magnetic fields these distances are larger (see Fig. 3 right panel). The small radius $r_{\max}$ of the region, which provides the dominant contribution to the observed diffuse flux of UHECR, imposes a constraint on the diffusion models, which will become more severe when/if particles with higher energies will be observed. As an example, let us consider the representative configuration (100 nG, 1 Mpc) and highest observed energy $E = 3 \times 10^{20}$ eV. In this case we have $E_c = 1 \times 10^{20}$ eV, $l_d(E) \approx 10$ Mpc and $l_{\mathrm{att}} = 21$ Mpc. To avoid rectilinear propagation from nearby sources we should impose the separation $d > l_d(E) \approx 10$ Mpc. For a maximum generation energy of $E_{\max} = 1 \times 10^{21}$ eV, the maximum distance is $r_{\max} < 70$ Mpc and is only marginally consistent with $d > 10$ Mpc. The UHECR sources at $r < 70$ Mpc with $d > 10$ Mpc and with maximum acceleration energy $E_{\max} \sim 1 \times 10^{21}$ eV tentatively imply AGN, whose luminosities satisfy the energy requirement for the observed UHECR fluxes in the case of weak magnetic fields. However, for the case of a weak GZK cutoff (diffusion in strong magnetic fields and large separation $d$) the required luminosities are very high $L_p \sim 10^{47}$ erg/s.

The calculated diffuse energy spectra are shown in Fig. 5 for the Bohm diffusion coefficient and for the complex generation energy spectrum (8). In case of configuration with a very strong magnetic gield (1000 nG, 1 Mpc, 30 Mpc) the spectrum has a weak GZK cutoff (the solid curve in Fig. 5). This spectrum agrees reasonably with the AGASA excess, but requires very large source luminosity $L_p = 1.5 \times 10^{47}$ erg/s. When magnetic field diminishes to 100 nG the GZK cutoff appears (dotted line), as it should according to the propagation theorem.

A weak GZK cutoff in the case of diffusive propagation is explained by the flux suppression at $E < E_{\mathrm{GZK}}$ cutoff due to longer propagation time from the source (see Section 6 for the detailed explanation).

The spectra calculated in this paper in the diffusion approximation are compatible, for the relevant parameters, with the numerical simulations in Yoshiguchi et al. (2003). As an example we present in Fig. 8 our spectra from a single source calculated in the diffusion approximation for magnetic configuration $(B_0,\ l_c)$=(100 nG, 1 Mpc) with the Kolmogorov spectrum of turbulence for a distance to the source of 10 Mpc (left panel) and 30 Mpc (right panel). For the distance 10 Mpc we also plot the spectrum for the rectilinear propagation shown by the dotted curve. The two curves intersect at $E_* \sim 3 \times 10^{20}$ eV, as they should provided by the condition $l_d(E) = r$, where $r$ is the distance to the source. At $E > E_*$ the particles propagate rectilinearly and the flux is given by the dashed line. This spectrum is compared with the numerical simulations of Yoshiguchi et al. (2003) for the same magnetic field configuration (Yoshiguchi (2004)), shown by the crosses. Since the calculations of Yoshiguchi et al. (2003) are not normalized, we equate the fluxes at energies with rectilinear propagation as shown in Fig. 8. One can observe considerable disagreement at $E \sim 8 \times 10^{19}$ eV, where it is possible to suspect a transitional regime between quasi-rectilinear and diffusive propagation in numerical simulations. For the distance to the source r=30 Mpc (right panel) the agreement is much better, probably because at these distances the diffusion regime is reached in the numerical simulations.

The study of this paper is not intended to be a realistic one. We consider the diffusive propagation of UHE particles

using an analytic approach with the aim of understanding the basic properties of propagation in strong magnetic fields. A realistic propagation should be studied within the hierarchical model of different magnetic fields in different large scale structures, as it is done in simulations (Sigl et al. (2003), Sigl et al. (2004), Dolag et al. (2003)). However, we are able to reach some practical conclusions.

Our study is focused on the spectra of UHECR. We demonstrated that the crucial parameter is the source separation $d$. For a wide class of magnetic field configurations, when the separation $d$ is smaller than the diffusion length $l_d$, the spectrum is universal, i.e. the same as in case of rectilinear propagation. For the simulation of Dolag et al. (2003) the spectrum must be universal. The simulations of Sigl et al. (2003), Sigl et al. (2004) and Yoshiguchi et al. (2003) include diffusive and intermediate regimes. According to our calculation, in the diffusion regime very strong magnetic fields, $B_0 \sim 1000$ nG, and large separation between sources are needed to produce a spectrum with weak (or absent) GZK cutoff. In this case very high source luminosities are required, $L_p > 1 \times 10^{47}$ erg/s. It disfavors diffusion in strong magnetic fields as the explanation for the AGASA excess at high energies.


## ACKNOWLEDGMENTS

We acknowledge participation of Askhat Gazizov at an early stage of this work. We are grateful to Vladimir Ptuskin for valuable discussion of diffusive propagation of UHECR and to Igor Tkachev for early discussion of hierarchical magnetic field structure of the universe and the possibility of quasi-rectilinear propagation of UHE protons. We acknowledge useful discussions with Pasquale Blasi and Yurii Eroshenko. We are grateful to the authors of the work Yoshiguchi et al. (2003), especially Hiroyuki Yoshiguchi and Katsuhiko Sato, for discussions and calculations made for comparison with our results. We also thank Richard Ford for a critical reading of the manuscript.
We thank the transnational access to research infrastructures (TARI) program trough the LNGS TARI grant contract HPRI-CT-2001-00149.


## APPENDIX

### SPECTRAL ENERGY DENSITY AND SCALE DEPENDENCE OF MAGNETIC FIELDS.

We shall derive here $\langle B^2 \rangle \propto k^{-s}$ from the spectral energy density of a turbulent plasma $w(k) \propto k^{-m}$. The turbulence is assumed to be described as an ensemble of hydromagnetic waves with wave numbers $\vec{k}$ and with vanishing mean electric field. The mean magnetic field on each scale $\lambda = 2\pi/k$ is $\langle \vec{B} \rangle_\lambda = \vec{B}_\lambda$. i.e. on the scale $\lambda$ the magnetic field is locally homogeneous. For the Alven waves the kinetic energy of turbulent fluid is equal to magnetic energy (Landau and Lifshitz (1987)).

Let us write down the Fourier expansion for the wave magnetic field. In the limit $u_A/c \ll 1$, where $u_A$ is the Alven velocity, $\omega/ku_A \ll 1$ and the magnetic fields can be considered as quasi-static. Here and below we shall omit the coefficients $(2\pi)^3$, which are inessential for our discussion.

$$\vec{B}(\vec{r},t) = \int d^3k \vec{B}(\vec{k},t) e^{i\vec{k}\vec{r}}$$
$$\vec{B}^*(\vec{r},t) = \int d^3k' \vec{B}^*(\vec{k}',t) e^{-i\vec{k}'\vec{r}} \tag{A1}$$

The energy of magnetic field in the normalizing volume $V$ is

$$W = \frac{1}{8\pi} \int d^3r \vec{B}(\vec{r},t) \vec{B}^*(\vec{r},t) \tag{A2}$$

Putting Eqs.(A1) into Eq.(A2) and using the definition of $\delta$ function

$$\int d^3r e^{i(\vec{k}-\vec{k}')\vec{r}} = \delta^3(\vec{k}-\vec{k}'), \tag{A3}$$

we obtain

$$W = \frac{1}{8\pi} \int d^3k |B(\vec{k},t)|^2. \tag{A4}$$

Assuming $B(\vec{k},t) = B(k,t)$ we find the energy density of waves and fluid as

$$w = \frac{1}{2V} \int dk\ k^2 B^2(k). \tag{A5}$$

The spectral energy density is then

$$w(k) = \frac{1}{2V} k^2 B^2(k). \tag{A6}$$

and hence for the Fourier component $B^2(k) \propto k^{-s_F}, \quad s_F = m+2$. Note that the Fourier component $B(k)$ does not have meaning of the magnetic field strength over the scale $k$; moreover the dimension of $B(k)$ is different from a magnetic field. The connection between $B_\lambda$, the average field on the scale $\lambda$, and the Fourier component $B(k)$, can be readily found from relation

$$w = \frac{1}{8\pi} B_\lambda^2 = \frac{1}{2V} \int_\lambda dk\ k^2 B^2(k)$$

where the integral is to be evaluated over region $\sim \lambda$. It results in

$$B_\lambda^2 \sim \frac{4\pi}{V} k^3 B^2(k) = 8\pi k w(k). \tag{A7}$$

Using the definition $B_\lambda^2 \propto k^{-s_\lambda}$, we obtain for the physical field $B_\lambda$, $s_\lambda = m - 1$, and $s_F - s_\lambda = 3$.

In particular, for the Kolmogorov spectrum we have $s_F = 11/3$ and $s_\lambda = 2/3$, and thus for deflection of UHE particles one should use the wave-number spectrum of magnetic fields in the form

$$B_\lambda^2 \propto k^{-2/3} \ . \tag{A8}$$

REFERENCES


L.A. Arzimovich and R.Z. Sagdeev, Physics of Plasma for Physicists (in Russian), Moscow, Atomizdat, 1979.
V.S. Berezinsky and S.I. Grigorieva, A & A **199** (1988) 1.
V.S. Berezinsky, V.A. Dogiel and S.I. Grigorieva, A&A **232**, 582 (1990a).
V.S. Berezinsky, S.V. Bulanov, V.A. Dogiel, V.L. Ginzburg, and V.S. Ptuskin, Astrophysics of Cosmic Rays, chapter IX, North-Holland (1990b).
V. Berezinsky, A.Z. Gazizov and S.I. Grigorieva (2002a), hep-ph/0204357.
V.S. Berezinsky, A.Z. Gazizov, and S.I. Grigorieva (2002b), astro-ph/0210095.
V. Berezinsky, A.Z. Gazizov and S.I. Grigorieva, hep-ph/0302483. Proc. of Int. Workshop "Extremely High Energy Cosmic Rays" (eds M.Teshima and T.Ebisuzaki), Universal Academy Press, Tokyo 63, 2003.
P. Blasi, S. Burles, A.V. Olinto, Ap.J. **514**, 79 (1999a).
P. Blasi and A.V. Olinto Phys. Rev. **D59** 023001 (1999b).
C.L. Carilli and G.B. Taylor, Annual Rev. Astr. Astroph., **40**, 319 (2002).
F. Casse, M. Lemoine, G. Pelletier Phys. Rev. **D65** 023002 (2002).
R. Davè, R. Cen, J.P. Ostriker, G.L. Bryan, L. Hernquist, N. Katz, D.H. Weinberg, M.L. Norman and B. O'Shea, Astrophys.J. 547 (2001) 574.
O. Deligny. A. Letessier-Selvon, E. Parizot, astro-ph/0303624.
K. Dolag, D. Grasso, V. Springel, I. Tkachev, astro-ph/0310902.
M. Giller, J. Wdowczyk, A.W. Wolfendale, J.Phys. G **6** 1561 (1980).
A.V. Glushkov and M.I. Pravdin, Astronomy Lett. **27**, 493 (2001).
D. Harari, S. Mollerach, E. Roulet, JHEP 0207 006 (2002).
N. Hayashida et al. (AGASA collaboration), Phys. Rev. Lett. **77** 1000 (1996).
N. Hayashida et al. (AGASA collaboration), Ap.J., **522**, 225 (1999).
C. Isola, M. Lemoine and G. Sigl, Phys. Rev. **D65** 023004 (2002).
A.N. Kolmogorov, Doklady Akad. Nauk. USSR, **30** 299 (1941).
R.N. Kraichnan, Phys. Fluids **8** 1385 (1965).
P.P. Kronberg, Rep. Progr. Phys. **57**, 325 (1994).
L.D. Landau and E.M. Lifshitz, Electrodynamics of Continuous Media, chapter VIII, Magnetic Hydrodynamics, Pergamon Press, 1987.
M. Lemoine, G. Sigl, P. Biermann, astro-ph/9903124.
E.M. Lifshitz and L.P. Pitaevskii, Physical Kinetics (v.10 of Theoretical Physics by L.D. Landau and E.M. Lifshitz) Fizmatlit 2001.
D. Ryu, H. Kang, P. Biermann, Astron. Astroph., **335**, 19 (1998).
G. Sigl, M. Lemoine, P. Biermann, Astrop. Phys. **10** 141 (1999).
G. Sigl, F. Miniati and T.A. Enßlin, Phys. Rev. **D68** 043002 (2003).
G. Sigl, F. Miniati and T.A. Enßlin, astro-ph/0401084.
D.N. Spergel et al (WMAP collaboration), Astrophys. J. Suppl. **148** (2003) 175.
T. Stanev et al, Phys. Rev. **D 62** 093005 (2000).
S.I. Syrovatskii, Sov. Astron. **3** 22 (1959).
P.G. Tinyakov and I.I. Tkachev, JETP Lett., **74** 445 (2001).
Y. Uchiori et al, Asrop. Phys. **13**, 157 (2000).
S.I. Vainstein, A.M. Bykov and I.N. Toptygin, Turbulence, Stream Layers and Shock Waves (in Russian), Nauka, Moscow (1989).
J.P. Vallee, Fund. Cosm. Phys. **19**, 1 (1997).
J. Wdowczyk, A.W. Wolfendale, Nature, **281**, 356 (1979).
H. Yoshiguchi, S. Nagataki, S. Tsubaki and K. Sato, Astrophys.J. 586 (2003) 1211-1231.
H. Yoshiguchi, private communication.